# Some performance results from NIRCam's coronagraphic prototype masks

Gopal Vasudevan[*], M. Reale[†], S. F. Somerstein[‡]

## ABSTRACT

The Near Infrared Camera (NIRCam) instrument for NASA's James Webb Space Telescope (JWST) is one of the four science instruments installed into the Integrated Science Instrument Module (ISIM) on JWST intended to conduct scientific observations over a five year mission lifetime. NIRCam's requirements include operation at 37 kelvins (K) to produce high resolution images in two wave bands encompassing the range from 0.6 microns to 5 microns. In addition NIRCam is used as a metrology instrument during the JWST observatory commissioning on orbit, during the initial and subsequent precision alignments of the observatory's multiple-segment 6.3 meter primary mirror. This paper describes some preliminary performance results of prototype coronagraph masks.

**Keywords:** NIRCam, James Webb, JWST, ISIM, Coronagraph Masks

## 1. INSTRUMENT OVERVIEW

The science objectives for the coronagraph are direct imaging and analysis of environments in the vicinity of nearby stars. These objectives require the development of methods for controlling the optical diffraction and scatter within high-dynamic-range space telescopes in order to conduct mission science for:

- Planetary systems and pre-conditions for life
- Detection of massive planets in orbit around stars
- Studies of circumstellar dust

The NIRCam instrument contains two mirror-image camera system modules mounted back-to-back. Figure 1.1 illustrates the optical layout of the coronagraph path of each module. The NIRCam spectral wavelength is divided into two optical channels on each of the two modules to provide a short wavelength channel from 0.6 microns to 2.3 microns, and a long wavelength channel covering 2.4 microns to 5.0 microns.

The coronagraph mask is placed off the NIRCam field of view. Thus to image the coronagraph field, a 4 degree wedge is placed at the re-imaged pupil plane. The Lyot stop is placed at the front face of this wedge. The coronagraph mask set contains 5 different masks and since there are two modules, there are a total of 10 different masks. Each mask comes with its own optimized Lyot stop.

Since JWST will have substantial sensitivity at longer wavelengths, the design of the coronagraph was chosen to be maximized at 3 and 4.6 microns (e.g. F335M and F460M) [Ref. 1]. To achieve this science, the coronagraph occulting masks and the attendant Lyot masks have to provide $10^{-4}$ contrast at 500 milli-arcsecs at 4.6 microns. A set of masks (Figure 1.2) were proposed for achieving the science. These include:

- Radial Gaussian
- Radial sinc$^2$
- Linear Gaussian
- Linear sinc$^2$
- Tapered linear sinc$^2$
- Third order masks

---

[*] contact: gopal.vasudevan@lmco.com, voice (650) 424-2118, fax (650) 424-3106
[†] contact: martina.j.reale@lmco.com, voice (408) 742-4564, fax (650) 354-5002
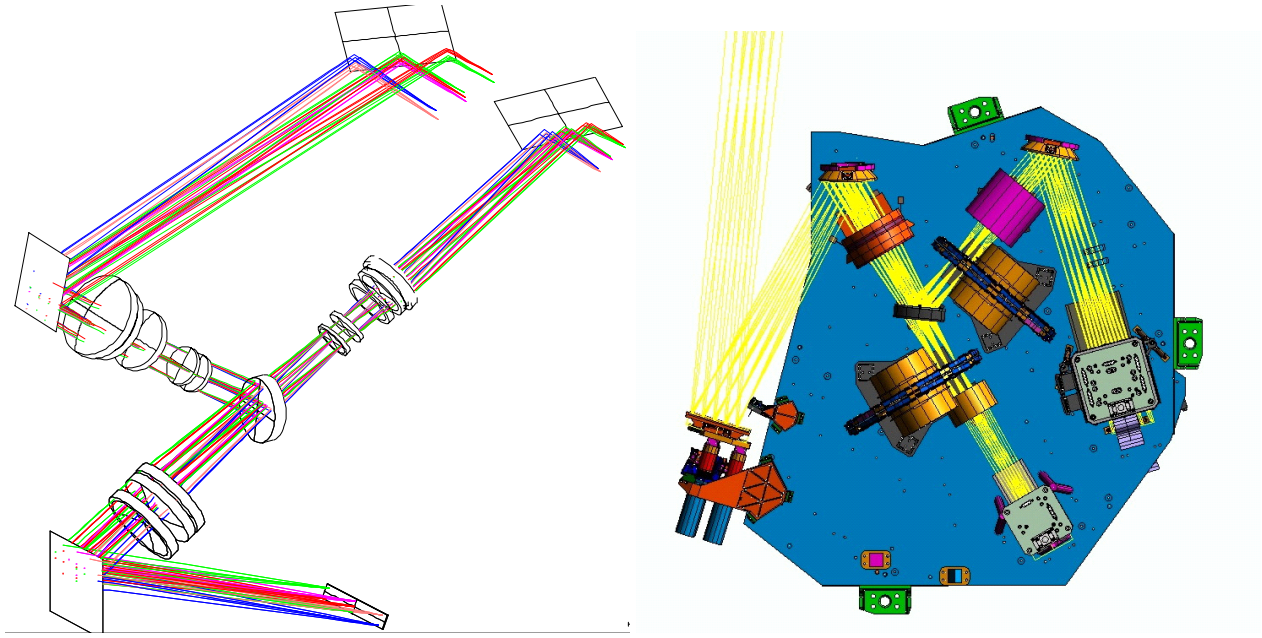[‡] contact: steve.somerstein@lmco.com, voice (650) 354-5077, fax (650) 354-5002

Figure 1.1: NIRCam Coronagraph Path Optical Layout

We investigated a binary dot matrix approach to fabricating these masks. In this paper we present some preliminary results of this approach.

## 2. DESCRIPTION OF THE MASKS

A mask is desired that has a specific density gradient as a function of position. This density pattern can be thought of as a grayscale. However, photolithography creates only binary (black or white) patterns which attach to a finite grid on the mask. This situation is similar to printing grayscale with only black ink on white paper. A pseudo grayscale can be created by varying the average dot density in local regions of the mask. This technique is called "halftoning". The halftoning technique being used is a variation of random thresholding. Thus, if the desired "transmission" at a specific location on the mask is less than some threshold value, write a black dot, otherwise write a white dot. The threshold value is selected at random for each specified grid location on the mask. Additional randomization approaches are possible and currently under investigation.

For each occulting mask shape, a binary pattern is generated. A glass substrate is coated with a thin uniform layer of masking material, for example chrome. Then using a photolithographic process, the binary pattern is imprinted onto
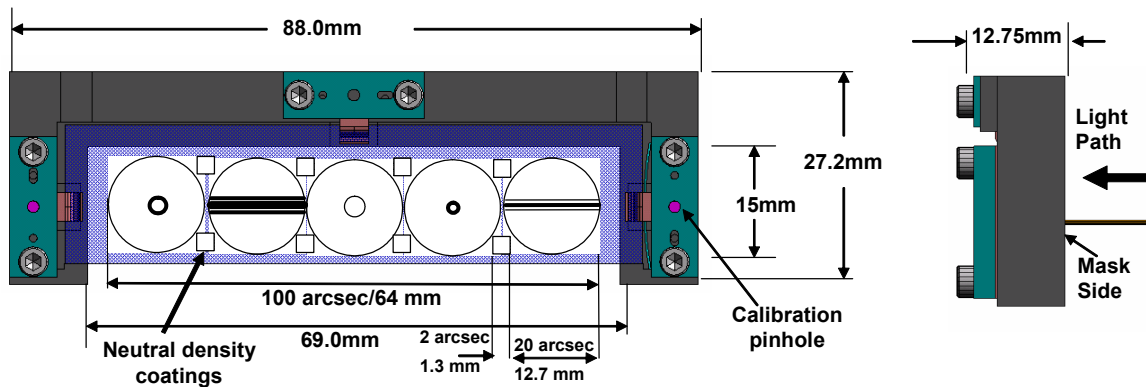

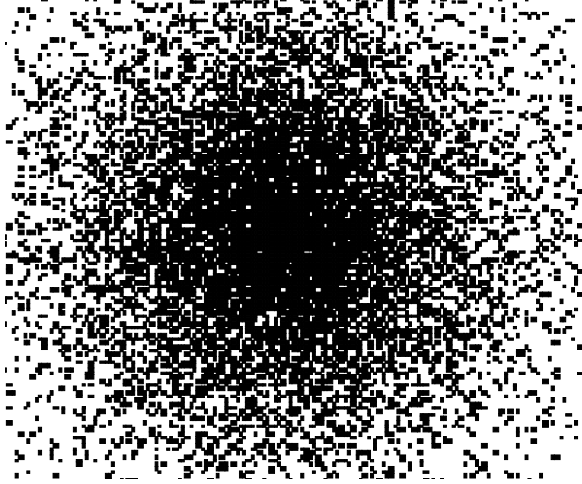Figure 1.2: An Occulting Mask Set
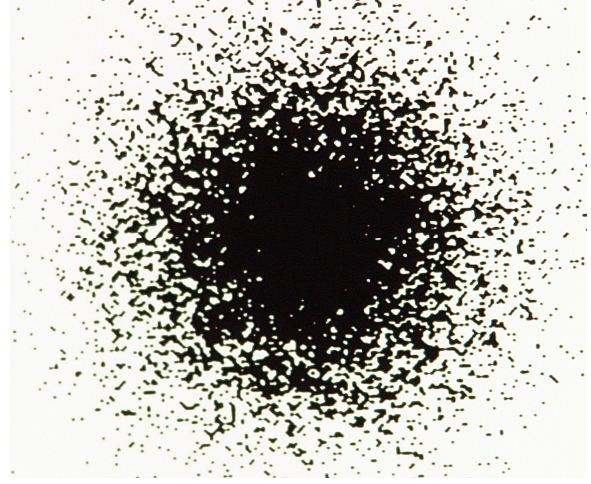
Figure 2.1: Gaussian Mask as Designed



Figure 2.2: Gaussian Mask as Fabricated

the substrate. Two approaches are possible. In one case, the photo-resist applied prevents the material from being etched away and in another it facilitates the removal. Both approaches lend themselves to different fabrication strategies and are appropriate for different types of masks. Figure 2.1 and Figure 2.2 show the designed and the as-fabricated masks.

## 3.  RESULTS

A sample test mask was analyzed using a pseudo vector propagation code DIFFRACT [Ref. 2, 3] to model the propagation past the dot matrix mask to provide a quick check on the performance. The mask used is a Gaussian profile with FWHM set to 70.2 μm, which corresponds to 6λF/# at an F number ratio of 18 at a wavelength of 650 nm. For the analysis we used an Optical density (OD) of the mask material to be 3.

The propagation model is a 4f optical system with the mask in the middle as shown below in Figure 3.1. The initial beam is unaberrated with uniform amplitude. The results as shown here are insensitive to polarization. The beam is propagated to the focus of the ideal lens and a mask function is applied. The mask function is a binary function, in which the transmission is reduced by the specified OD value of each dot. The masks as fabricated are of OD3, so the transmission is 0.1%. Since the mask function works with amplitude rather than with intensity, each dot is provided a transmissivity factor of 0.032. After transmitting through the mask the beam has only 13.3% of its original power. The power is distributed within several random hot spots loosely forming an annulus with radii values similar to that of the 1st zero of the Airy disk. The beam is next propagated to the collimating lens. For this simulation an aperture function is applied at the collimating lens. The beam is collimated and propagated to the Lyot plane. Figure 3.2 shows the
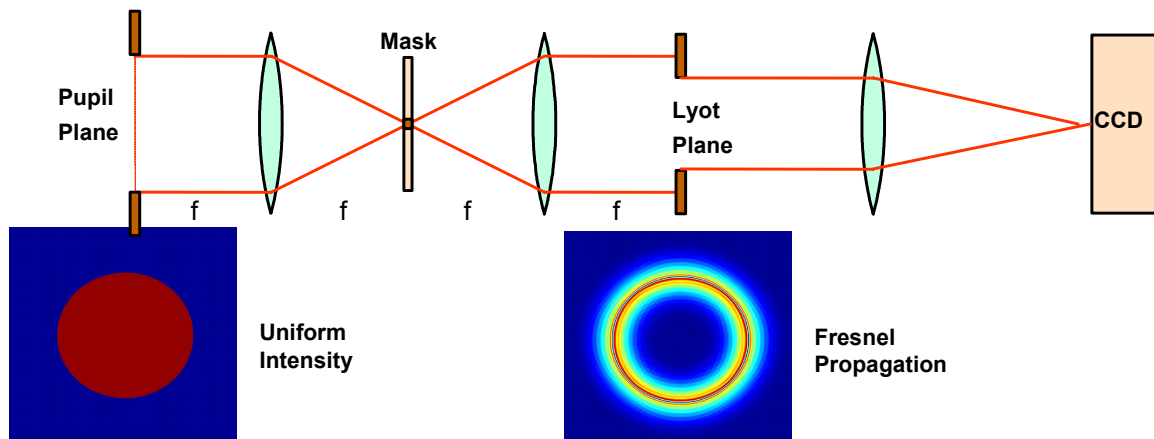


Figure 3.1: Propagation model with approximate representations of the beam at the pupil and at the Lyot planes
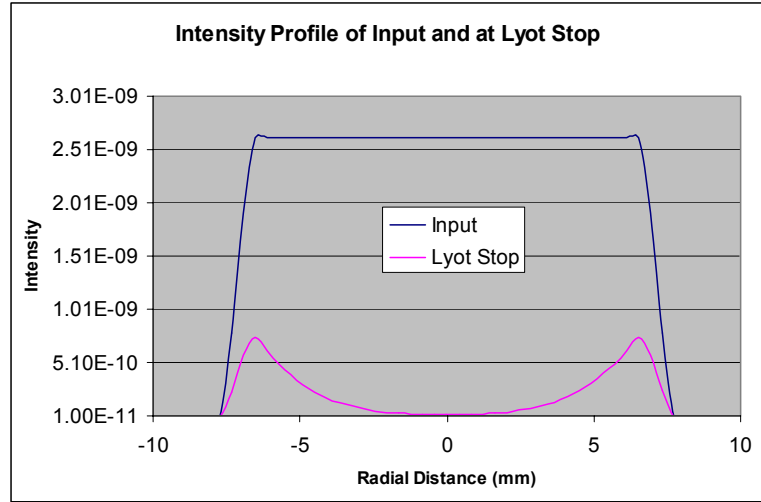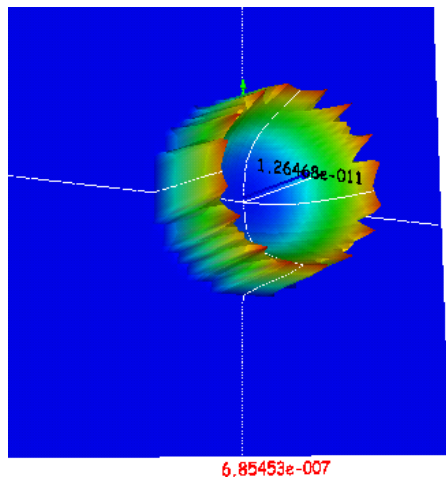
Figure 3.2: Modeling Results for a Gaussian Coronagraph Mask with OD 3

intensity profile at the Lyot plane. The simulation assumes perfect anti-reflection without taking into account any coatings. The results show that with an OD of 3, the max contrast is about 1e-03.

A 4f optical system with an imaging lens was constructed in the lab. A laser diode (635nm) light source was used at below threshold current setting giving approximately about 50nm of wavelength band. Data was taken with and without the mask in place. The dark removed data was recorded. The peak intensity ratio showed a 1e-02 max contrast. The discrepancy comes mainly from residual aberrations in the test setup. The masks were not anti-reflection coated at the time of these tests. The Lyot stop intensity is shown in Figure 3.3. The intensity at the Lyot stop including the mask is less than the camera noise floor as evidenced by the near flat profile of the beam. Further work is being performed to improve the test data so as to characterize the masks. The effect of the ghost reflections was noticeable using a top hat mask as shown in Figure 3.4
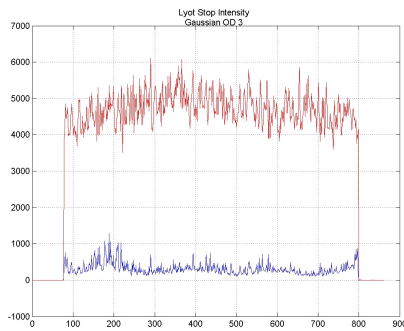


Figure 3.3: Lyot Stop Intensity Profile for Gaussian Mask OD 3
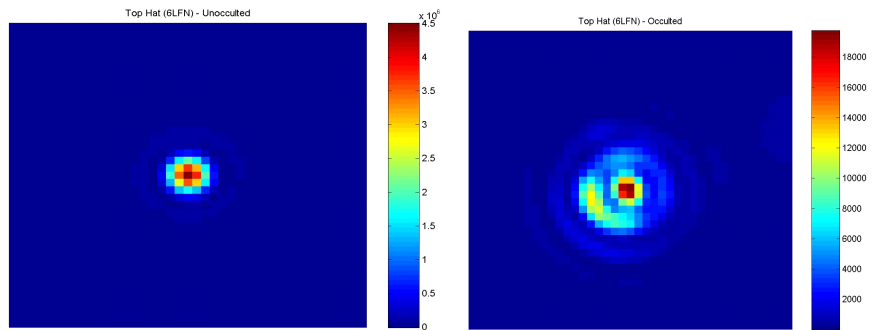
Figure 3.4: Results from a Top Hat Coronagraph Mask

## 4. CONCLUDING REMARKS

Detailed coronagraph fabrication requirements are being defined. Preliminary results show that the fabrication techniques for these masks are promising.

## 5. REFERENCES

1. Beichman, C., Trauger, J., Green, J.J., "Initial Assessment of Performance of NIRCAM Coronagraph," JWST *Engineering Memorandum*, June 2004.
2. MM Research, Inc., "Guide to Program DIFFRACT (8.2)," March 2004
3. Mansuripur, M., "Certain computational aspects of vector diffraction problems," JOSA A, Vol. 6, No. 5, June 1989, pp 786-805.